OPEN

Citation: Cell Death and Disease (2013) 4, e615; doi:10.1038/cddis.2013.128
© 2013 Macmillan Publishers Limited All rights reserved 2041-4889/13
www.nature.com/cddis

ATM-NFκB axis-driven TIGAR regulates sensitivity of glioma cells to radiomimetics in the presence of TNFα

S Sinha[1], R Ghildiyal[1], VS Mehta[2] and E Sen*[,1]

Gliomas are resistant to radiation therapy, as well as to TNFα induced killing. Radiation-induced TNFα triggers Nuclear factor κB (NFκB)-mediated radioresistance. As inhibition of NFκB activation sensitizes glioma cells to TNFα-induced apoptosis, we investigated whether TNFα modulates the responsiveness of glioma cells to ionizing radiation-mimetic Neocarzinostatin (NCS). TNFα enhanced the ability of NCS to induce glioma cell apoptosis. NCS-mediated death involved caspase-9 activation, reduction of mitochondrial copy number and lactate production. Death was concurrent with NFκB, Akt and Erk activation. Abrogation of Akt and NFκB activation further potentiated the death inducing ability of NCS in TNFα cotreated cells. NCS-induced p53 expression was accompanied by increase in TP53-induced glycolysis and apoptosis regulator (TIGAR) levels and ATM phosphorylation. siRNA-mediated knockdown of TIGAR abrogated NCS-induced apoptosis. While DN-IκB abrogated NCS-induced TIGAR both in the presence and absence of TNFα, TIGAR had no effect on NFκB activation. Transfection with TIGAR mutant (i) decreased apoptosis and γH2AX foci formation (ii) decreased p53 (iii) elevated ROS and (iv) increased Akt/Erk activation in cells cotreated with NCS and TNFα. Heightened TIGAR expression was observed in GBM tumors. While NCS induced ATM phosphorylation in a NFκB independent manner, ATM inhibition abrogated TIGAR and NFκB activation. Metabolic gene profiling indicated that TNFα affects NCS-mediated regulation of several genes associated with glycolysis. The existence of ATM-NFκB axis that regulate metabolic modeler TIGAR to overcome prosurvival response in NCS and TNFα cotreated cells, suggests mechanisms through which inflammation could affect resistance and adaptation to radiomimetics despite concurrent induction of death.

Cell Death and Disease (2013) **4,** e615; doi:10.1038/cddis.2013.128; published online 2 May 2013
Subject Category: Cancer Metabolism

Glioblastoma multiforme (GBM) – the most aggressive malignant brain tumor, is largely resistant to current therapeutic modalities, including radiotherapy. Nuclear factor κB (NFκB) is activated by ionizing radiation,[1] and irradiation induced NFκB mediates radiation-resistance in glioma cells through defense against oxidative stress.[2] The resistance of several tumors to TNFα-induced apoptosis[3] has been attributed to TNFα-mediated NFκB activation.[4,5] NFκB inhibition sensitizes melanoma cells to a natural radiomimetic Neocarzinostatin (NCS)-induced apoptosis in response to aberrant TNF receptor associated factor 2 (TRAF2) signaling.[6] Radiation-induced TNFα-NFκB cross-talk promotes survival in neuroblastoma cells.[7] TNFα-mediated selection of breast cancer cells with stably acquired inducible NFκB activity, confers them resistance to irradiation or TNFα-induced killing.[8]

NCS induces cell death by triggering reactive oxygen species (ROS).[9] We have previously shown that ROS sensitizes glioma cells to chemotherapeutics.[10,11] p53 accumulates in response to ROS stress[12] and p53-induced glycolysis, and apoptosis regulator (TIGAR) protects cells from ROS-associated apoptosis.[13] Abrogation of TIGAR sensitizes glioma cells to radiation,[14] and TIGAR protects glioma cells from ROS-mediated apoptosis.[15] Importantly, TIGAR is a regulator of glycolysis,[13] and targeting key metabolic enzymes modulating glycolysis is considered a novel therapeutic approach for the highly glycolytic GBM.[16,17] Besides, NFκB maintains balance between glycolysis and mitochondrial respiration by regulating energy metabolism networks.[18]

Ataxia telangiectasia mutated (ATM) protein kinase – the master regulator of response to double-strand breaks (DSBs), links DNA damage response (DDR) and signaling events associated with proliferation and apoptosis in NCS-treated cells.[19] Also, ATM sustains NFκB activation following DNA damage.[20] As we have shown that inhibition of NFκB by chemotherapeutics sensitizes glioma cells to TNFα-induced apoptosis,[21,22] we investigated whether TNFα effects the responsiveness of glioma cell to NCS by fine tuning the balance between survival and death through regulation of key apoptotic and metabolic network. This study forges the first link between NFκB, TIGAR and ATM in regulating responsiveness of glioma cells to radio-mimietic in the presence of proinflammatory cytokine TNFα.

[1]Cellular and Molecular Neuroscience Division, National Brain Research Centre, Manesar, Haryana, India and [2]Paras Hospitals, Gurgaon, Haryana, India
*Corresponding author: E Sen, Cellular and Molecular Neuroscience Division, National Brain Research Centre, Nainwal Mode, Manesar, Gurgaon, Haryana 122050, India. Tel: +91 12 4284 5235; Fax: +91 12 4233 8910/28; E-mail: ellora@nbrc.ac.in
Keywords: TIGAR; ATM; TNFα; NFκB; neocarzinostatin
Abbreviations: ATM, Ataxia telangiectasia mutated; DN-IκB, Dominant Negative Inhibitor of kappa B; FBPase, Fructose bisphosphatase; GBM, Glioblastoma multiforme; HK2, Hexokinase 2; NCS, Neocarzinostatin; PDK, Pyruvate dehydrogenase kinase; TIGAR, TP53 induced glycolysis and apoptosis regulator
Received 02.11.12; revised 07.3.13; accepted 15.3.13; Edited by C Munoz-Pinedo

Results

TNFα enhances NCS-mediated glioma cell death. To evaluate the effect of NCS on glioma cell viability, A172 and U87MG cells were treated with different concentration of NCS for 24 h. A ~40% reduction in viability was observed in NCS-treated glioma cells irrespective of the dose of treatment (Figure 1a). As death induced by different doses of NCS was comparable (Figure 1a), we chose 1 μg/μl of NCS for subsequent treatments. While TNFα alone had no effect on viability of glioma cells, cotreatment with NCS resulted in ~50–65% decrease in viability at 24 h, as compared with control (Figure 1b). Thus, TNFα enhances NCS-induced glioma cell death.

NCS-mediated death involves Caspase-9 activation. As NCS-induced apoptosis in breast cancer cells involves caspase-9 activation,[23] its involvement in NCS-induced glioma cell death was investigated. Cleaved caspase-9 level was elevated in NCS-treated cells both in the presence and absence of TNFα (Figure 1c). As NCS-induced apoptosis involves cytochrome *c*[23] and as pro-apoptotic protein BAX promotes the release of cytochrome *c* from mitochondria,[24] the levels of BAX and cytochrome *c* in NCS-treated cells was determined. NCS increased BAX, BAD and cytochrome *c* expression both in the presence and absence of TNFα (Figure 1c). To further confirm the role of caspase-9 in NCS-mediated death, viability of cells treated with different combinations of TNFα and NCS in the presence and absence

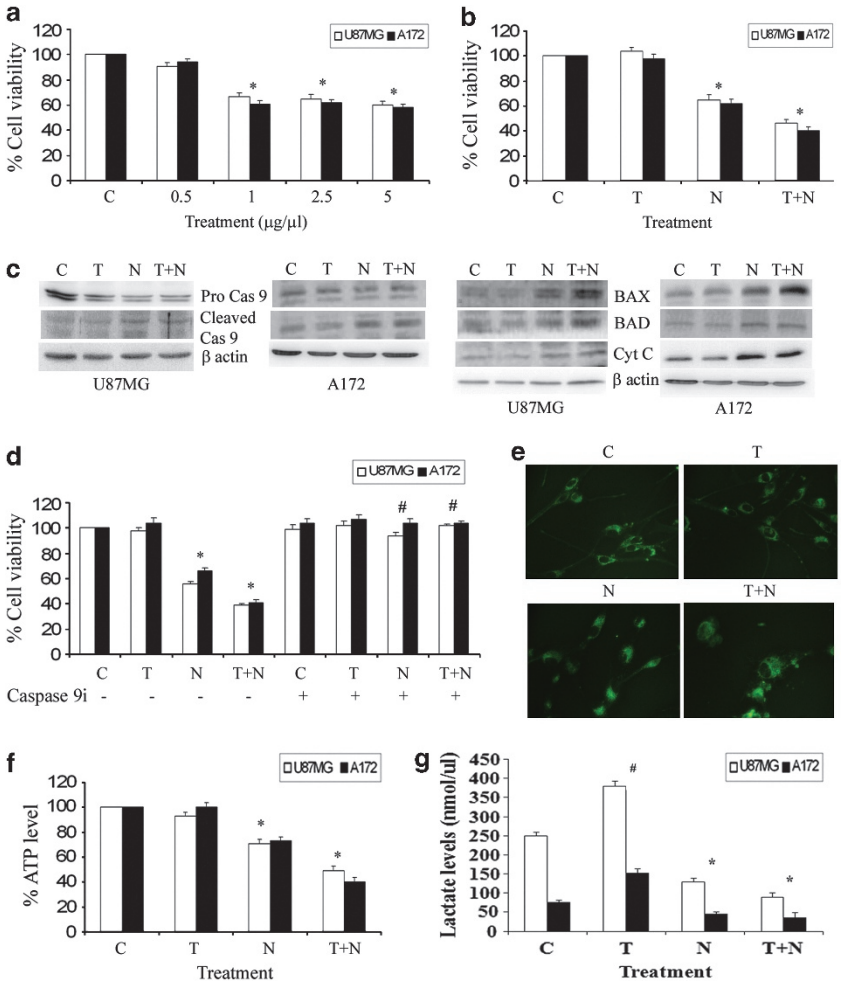

Figure 1 NCS-induced glioma cell death is caspase-9 dependent and involves mitochondria. (**a**) Viability of glioma cells treated with different concentration of NCS for 24 h as determined by MTS assay. (**b**) Viability of glioma cells treated with 1 μg/μl NCS in the presence and absence of TNFα (50 ng/ml) for 24 h as determined by MTS assay. (**c**) Western blot of cleaved caspase-9, Bad, Bax and Cytochrome *c* in glioma cells treated with different combinations of NCS and TNFα. A representative blot is shown from three independent experiments with identical results. Blots were reprobed for β-actin to establish equivalent loading. (**d**) Viability of glioma treated with different combinations of TNFα and NCS in the presence and absence of Caspase-9 inhibitor, as determined by MTS assay. The graph (**a**, **b**, **d**) represents the viable glioma cells percentage of control. * denotes significant change from control ($P<0.05$). #denotes significant change from NCS and NCS + TNFα ($P<0.05$). (**e**) Compromised mitochondrial integrity in NCS-treated cells both in the presence and absence of TNFα, as demonstrated by MitoTracker green staining. Cells treated with different combinations of NCS and TNFα were stained with MitoTracker green FM and examined at × 40 magnification. (**f**) Intracellular ATP content of glioma cells treated with different combinations of NCS and TNFα.* denotes significant change from control ($P<0.05$). (**g**) NCS decreases lactate production in glioma cells both in the presence and absence of TNFα. Graph indicates lactate levels in cells treated with different combinations of NCS and TNFα. Values represent the means ± S.E.M. from three independent experiments. #denotes significant change from control ($P<0.05$). *denotes significant change from TNFα ($P<0.05$)

of caspase-9 inhibitor was determined. The ability of caspase-9 inhibitor to revert the cytotoxic effect of NCS indicated the involvement of caspase-9 in NCS-mediated apoptosis (Figure 1d).

NCS disrupts mitochondrial morphology and decreases ATP generation. As elevated cytochrome *c* in NCS-treated cells is suggestive of mitochondrial dysfunction, MitoTracker green staining, which allows visualization of healthy functional mitochondria was performed. NCS disrupted mitochondrial morphology both in the presence and absence of TNFα (Figure 1e). Mitochondrial oxidation is one of the key mitochondrial functions involved in ATP synthesis. As NCS-induced glioma cell death involved mitochondria, ATP levels in NCS-treated cells was determined. The ~20% decrease in ATP generation observed in NCS-treated cells was further reduced by 40–50% in the presence of TNFα. Thus, NCS-mediated decrease in energy homeostasis is heightened in the presence of TNFα (Figure 1f).

NCS decreases lactate accumulation. Elevated lactate levels contribute to radioresistance.[25] As lactate is an important contributor to ATP generation in astrocytoma cells,[26] lactate levels in NCS-treated cells with diminished ATP levels were determined. NCS decreased lactate production both in the presence and absence of TNFα (Figure 1g).

NCS-mediated enhanced NFκB activation in TNFα-treated cells confers prosurvival advantage. NFκB is activated by ionizing radiation.[1] Besides, NFκB regulates mitochondrial respiration and has a role in metabolic adaptation in cancer.[18] As NCS-induced glioma cell death involved mitochondria, the status of NFκB activity in NCS-treated cells was determined. Though NCS had no significant effect on NFκB activity, it significantly enhanced TNFα mediated increase in NFκB transcriptional activity (Figure 2a). Thus, NCS-potentiated TNFα induced aberrant NFκB activation in glioma cells.

We have shown that chemotherapeutics mediated abrogation of TNFα induced NFκB activation, sensitizes glioma cell to TNFα induced apoptosis.[21,22] To explain the incongruity of increased NFκB activation in cells undergoing death, the ability of NCS to induce death in cells transfected with IκBM was investigated. While transfection with IκBM increased NCS-induced death, this increase was significantly greater in cells cotreated with NCS and TNFα. This indicated that inhibition of NFκB activation increases sensitivity of glioma cells to NCS induced death in the presence of TNFα (Figure 2b).

NCS increases Akt and Erk phosphorylation. Akt activates NFκB to suppress apoptosis[27] and inhibition of mitochondrial respiration induces Akt activation.[28] Coactivation and mutual dependence of ERK and NFκB enhances cell survival after irradiation exposure.[29] As NCS-induced disruption of mitochondrial integrity was accompanied by elevated NFκB activation, the effect of NCS on Akt and Erk activation was investigated. NCS and TNFα cotreatment

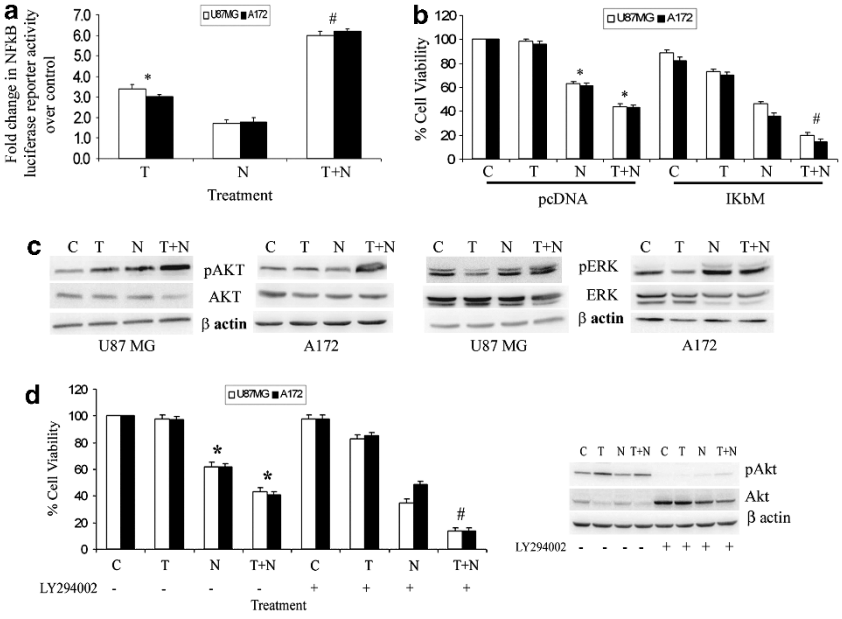

Figure 2 NCS-induced NFκB, Akt and Erk, activation regulates prosurvival response in the presence of TNFα. (**a**) NCS increases TNFα-induced NFκB activation in glioma cells. The graph represents fold change in NFκB luciferase activity over control, in cells treated with TNFα or NCS or both for 24 h. Values represent the means ± S.E.M. from three independent experiments. * denotes significant change from control, #denotes significant change from TNFα-treated cells ($P<0.05$). (**b**) NCS-mediated cell death in the presence and absence of TNFα is increased in cells transfected with IκBM. Viability of mock transfected or IκBM transfected glioma cells treated with different combinations of TNFα and NCS, was determined by MTS assay. (**c**) Western blot analysis indicating Akt and Erk phosphorylation in glioma cells treated with TNFα or NCS or both for 24 h. Representative blot is shown from three independent experiments with identical results. Blots were reprobed with β-actin to establish equivalent loading. (**d**) Treatment with Akt inhibitor enhances NCS-induced glioma cell death. Viability of glioma treated with different combinations of TNFα and NCS in the presence and absence of Akt inhibitor LY294002, as determined by MTS assay. (Inset) Akt inhibitor abrogates pAkt levels in cells treated with different combinations of TNFα and NCS as determined by western blot analysis. The graph (**b**, **d**) represents viable glioma cells expressed as percentage of control. Values (**b**, **d**) represent the means ± S.E.M. from three independent experiments. * denotes significant change from control, #denotes significant change from mock transfected (**b**) or NCS + TNFα (**d**) ($P<0.05$)

increased pAkt and pErk levels in glioma cells (Figure 2c). Increase in Erk phosphorylation was also observed in A172 cells treated with NCS alone (Figure 2c).

Activated Akt is associated with prosurvival responses in glioma. To establish the functional significance of this increased Akt activation in NCS and TNFα cotreated cells undergoing death, the viability of these cells in the presence of Akt inhibitor LY294002 was determined. Though inhibition of Akt resulted in increased sensitization of glioma cells to NCS-mediated cell death, sensitization was significantly greater in the presence of TNFα (Figure 2d). This suggests that aberrant Akt activation prevents the maximal induction of cell death by NCS (Figure 2d).

Increased p53 expression and ROS generation in NCS-treated cells. NFκB cooperates with p53 to regulate bioenergetic pathway controlling adaptation to metabolic stress.[18] As NFκB-p53 cross-talk affect tumor-associated metabolic changes and transformation,[30] p53 status in NCS and TNFα cotreated cells with heightened NFκB activation was determined. NCS increased p53 phosphorylation (Ser-15), as well as total p53 level both in the presence and absence of TNFα (Figure 3a). p53 accumulation in response to ROS facilitates cellular responses to ROS-induced DNA damage.[12] As NCS-mediated ROS induces cell death[9] the status of ROS in NCS-treated cells was determined. NCS elevated ROS generation in glioma cells (Supplementary Figure 1a). The ability of ROS inhibitor NAC to abrogate NCS-induced cytotoxicity, both in the presence and absence of TNFα, suggested that NCS-induced cell death is ROS dependent (Supplementary Figure 1b).

NCS elevates TIGAR levels in the presence and absence of TNFα. By simultaneously regulating glycolysis, apoptosis and ROS generation, TIGAR regulates oxidative mitochondrial metabolism.[13] p53 not only induces apoptosis but by activating TIGAR it also contributes to metabolic abnormalities.[31] Besides, knockdown of TIGAR radiosensitizes glioma cells.[14] *In silico* analysis Oncomine based on cancer microarray database and integrated data-mining platform indicated elevated TIGAR in GBM.[15] On investigating the status of TIGAR in GBM tumors, heightened TIGAR expression was observed in glioma tumors as compared with the surrounding normal tissue (Figure 3b). As NCS-induced glioma cell death involves mitochondrial dysfunction, elevated ROS and p53 activation; the status of TIGAR in these cells was investigated. While TIGAR levels in control and TNFα-treated cells were comparable (Figure 3c), NCS elevated TIGAR levels both in the presence and absence of TNFα (Figure 3c).

TIGAR regulates NCS-mediated cell death. TIGAR modulates the apoptotic responses to p53.[13] To investigate the functional significance of increased TIGAR levels in regulating apoptosis in NCS-treated cells with elevated p53 levels, the viability of NCS-treated glioma cells transfected with TIGAR siRNA was determined. NCS induced cell death both in the presence and absence of TNFα was significantly reduced upon siRNA-mediated knockdown of TIGAR (Figure 4a). Decrease in TIGAR expression reduced the sensitivity of glioma cells to NCS-induced apoptosis.

Functioning in a manner similar to FBPase-2, TIGAR lowers Fru-2, 6-P2 levels thereby decreasing the activity of

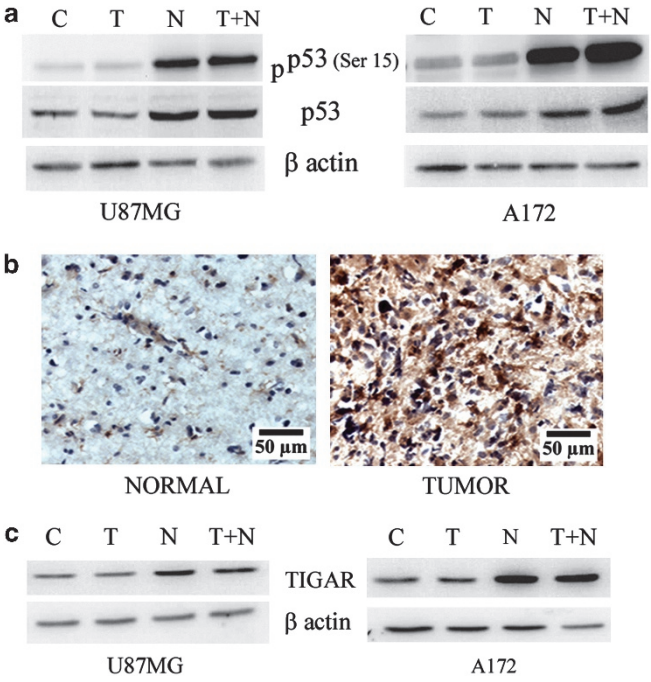

Figure 3 NCS increases p53 and TIGAR expression in glioma cells. (**a**) Western blot indicating increased phosphorylated and total p53 levels in cells treated with NCS in the presence and absence of TNFα. (**b**) IHC of TIGAR in glioma tumor and surrounding normal tissue as revealed by IHC (× 40 magnification). (**c**) NCS increases TIGAR expression in the presence and absence of TNFα, as demonstrated by western Blot analysis. Figure (**a**, **c**) representative blot shown from three independent experiments with identical results. Blots were reprobed with β-actin to establish equivalent loading

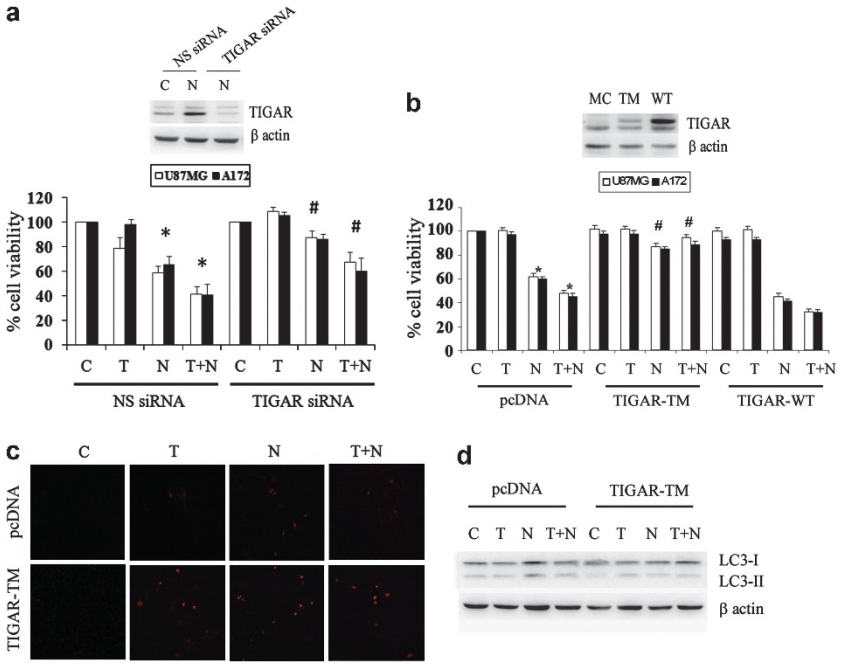

Figure 4 NCS-induced TIGAR regulates viability and ROS production in glioma cells. (**a**) siRNA-mediated knockdown of TIGAR abrogates NCS-induced decrease in glioma cell viability as determined by MTS assay. The graph represents the viable glioma cells percentage of control, transfected with TIGAR siRNA when treated with NCS in the presence and absence of TNFα for 24 h. Inset shows the knockdown efficiency of TIGAR siRNA. (**b**) The viability of glioma cells transfected with TIGAR-WT or TIGAR-TM and treated with NCS or TNFα or both for 24 h, was determined by MTS assay. The graph represents percentage viable cells of control. Inset shows the TIGAR levels upon transfection of TIGAR-WT and TIGAR-TM as determined by western blot. Values in (**a**, **b**) represent the means ± S.E.M. from three independent experiments. *denotes significant change from control, #denotes significant change from NCS and NCS + TNFα ($P<0.05$). (**c**) The images depict ethidium fluorescence in cells treated with different combinations of NCS and TNFα, resulting from oxidation of DHE by ROS. A greater ethidium fluorescence was observed in TIGAR-TM transfected U87MG cells treated with NCS both in the presence and absence of TNFα as compared with mock transfected cells. (**d**) TIGAR does not affect LC3-II expression in NCS-treated glioma cells. Western blot analysis indicating LC3-II levels in mock transfected and TIGAR-TM transfected U87MG glioma cells treated with NCS or TNFα or both for 24 h. Figure is a representative blot shown from three independent experiments with identical results. Blots were reprobed with β-actin to establish equivalent loading

phosphofructokinase-1 (PFK-1) and enhancing the activity of FBPase-1, to subsequently inhibit glycolysis.[13] As decreased glycolysis enhances cell death by apoptosis,[32] we further investigated the role of TIGAR in sensitizing glioma cells to NCS-induced death in the backdrop of its ability to regulate glycolysis. The viability of cells transfected with TIGAR-WT or TIGAR-TM (altered in the key residues essential for bisphosphatase activity), and treated with different combinations of NCS and TNFα was determined. Though silencing of TIGAR induces glioma cell apoptosis,[14] we failed to observe any significant change in glioma cell viability upon transfection with either TIGAR-WT or TIGAR-TM. It is possible that the cell context determines response of TIGAR to different stimuli.

While transfection with TIGAR-WT increased NCS-induced death by ~10–15% (Figure 4b), transfection with TIGAR-TM abrogated NCS-mediated cell death both in the presence and absence of TNFα (Figure 4b). An ~80% inhibition of NCS-induced death was observed in cells transfected with TIGAR-TM. On the other hand, TIGAR-WT or TM had no effect on the viability of cells in the absence of NCS or TNFα. Though TIGAR-TM exhibits impaired anti-apoptotic activity,[13] its effect on cell survival is known to be both cell and context dependent.[13] Along with TIGAR siRNA results, ability of TIGAR-TM to abrogate NCS-induced death indicated the involvement of TIGAR in sensitizing glioma cells to NCS-mediated apoptosis.

TIGAR regulates intracellular ROS levels in NCS-treated cells. As TIGAR protect cells from ROS-associated apoptosis,[13] we investigated whether TIGAR regulates intracellular ROS to effect NCS-induced apoptosis. Transfection of U87MG cells with TIGAR-TM increased ROS in NCS-treated cells both in the presence and absence of TNFα (Figure 4c). Similar results were observed with A172 (data not shown). This indicated that elevated TIGAR protects glioma cells from NCS- and TNFα-induced ROS.

NCS has no effect on LC3-II expression. Induction of autophagy upon loss of TIGAR moderates apoptotic response by restraining ROS levels.[33] To explain the paradox between enhanced ROS levels and increased survival in TIGAR-TM-transfected cells despite NCS mediated death being ROS dependent, the expression of autophagic marker LC3-II in TIGAR-TM-transfected cells treated with NCS was determined. Conversion of LC3-I to LC3- II which indicates induction of autophagy,[34] remained unaffected in NCS-treated cells both in the presence and absence of TNFα. NCS-induced glioma cell death does not involve autophagy, as LC3-II expression in NCS-treated cells between mock transfected and TIGAR-TM-transfected cells were comparable (Figure 4d).

NFκB regulates NCS-induced TIGAR expression but Akt has no effect. To explain the dichotomy of coexistence of

both pro-and antiapoptotic signals in cells undergoing death, role of NFκB and Akt in regulating TIGAR was investigated. While transfection with IκBM decreased TIGAR levels in NCS-treated cells both in the presence and absence of TNFα, the decrease was greater in cells cotreated with NCS and TNFα. However, NFκB inhibition had no effect on basal TIGAR levels in untreated or TNFα-treated cells (Figure 5a). On the other hand, Akt inhibition had no effect on NCS-induced TIGAR levels both in the presence and absence of TNFα (Figure 5a).

TIGAR regulates Akt and Erk phosphorylation but has no effect on NFκB activation in NCS-treated cells. The ability of TIGAR-TM to inhibit the apoptotic ability of NCS, prompted us to investigate its role in regulating Akt and Erk activation. Transfection with TIGAR-TM further elevated NCS-induced antiapoptotic regulator Akt and Erk (Figure 5b). This could possibly account for reversal of NCS-mediated death in TIGAR-TM transfected cell despite an increase in proapoptotic ROS. As NFκB positively regulates TIGAR in cells cotreated with NCS and TNFα, we questioned whether TIGAR is involved in sustaining elevated NFκB in these cells. The ability of NCS to increase TNFα-induced NFκB activation remained unaffected in cells transfected with TIGAR-TM (Figure 5c). Therefore, increase in TNFα-induced NFκB activation in NCS-treated cells is independent of TIGAR.

TIGAR affects p53 and its target gene p21 in NCS-treated cells. NCS induced increase in p53 and its target p21 levels, both in the presence and absence of TNFα, and was abrogated in cells transfected upon with TIGAR-TM. This decrease in p53 correlated with TIGAR-TM mediated reversal of NCS-induced apoptosis (Figure 5d).

NCS-induced ATM phosphorylation regulates NFκB activation in TNFα-treated cells. Activation of ATM in response to ionizing radiation is Akt dependent.[35] As ATM elicits DDR (DNA damage response) that confers radio-resistance in glioma,[36] we determined ATM status in NCS-treated cells with elevated Akt levels. NCS increased ATM phosphorylation both in the absence and presence of TNFα (Figure 6a). ATM regulates NFκB in response to genotoxic stress.[37] As increased ATM phosphorylation in NCS and TNFα cotreated cells is concurrent with elevated NFκB activation, the effect of ATM inhibition on NFκB activation was determined. NFκB activation in TNFα-treated cells both in the presence and absence of NCS was abrogated by ATM inhibitor (Figure 6b). This supports previous findings that

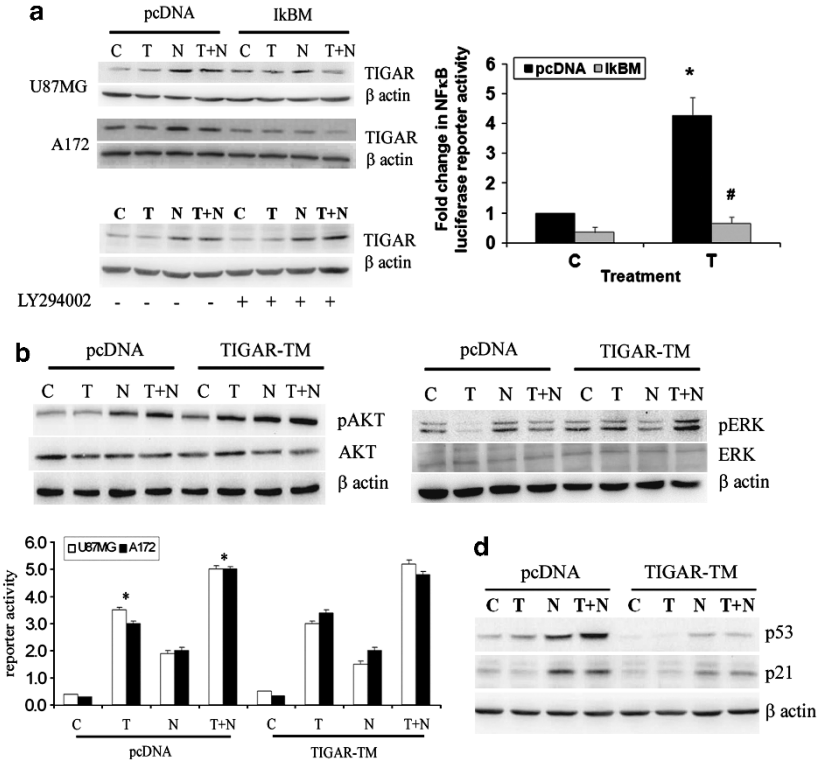

Figure 5 NFκB-dependent NCS induced TIGAR regulates Akt/Erk activation in the presence of TNFα. (**a**) NFκB regulates TIGAR but Akt has no effect. Western blot demonstrates TIGAR level cells treated with Akt inhibitor or transfected with IκBM and treated with NCS or TNFα or both. Inset indicating specificity of IκBM as demonstrated by decrease in TNFα induced NFκB luciferase reporter activity in cells transfected with IκBM as compared with mock transfected control. *denotes significant change from control ($P<0.05$). #denotes significant change from TNF ($P<0.05$). (**b**) TIGAR negatively regulates Akt and Erk phosphoryation in NCS-treated U87MG cells. Western blot of phosphorylated Akt and Erk in mock transfected or TIGAR-TM transfected glioma cells treated with NCS or TNFα or both. (**c**) TNFα-induced activation of NFκB is independent of TIGAR. NFκB transcriptional activation in cells cotransfected with NFκB luciferase reporter and TIGAR-TM, and treated with NCS in the presence and absence of TNFα. Graph indicates fold change in luciferase reporter activity over control. *denotes significant change from TNF ($P<0.05$). (**d**) TIGAR regulates p53 and its target p21. Western blot analysis indicating p53 and p21 levels in mock transfected and TIGAR-TM transfected U87MG glioma cells treated with NCS or TNFα or both for 24 h. Figures (**a**, **b** and **d**) representative blot shown from three independent experiments with identical results. Blots were reprobed with β-actin to establish equivalent loading

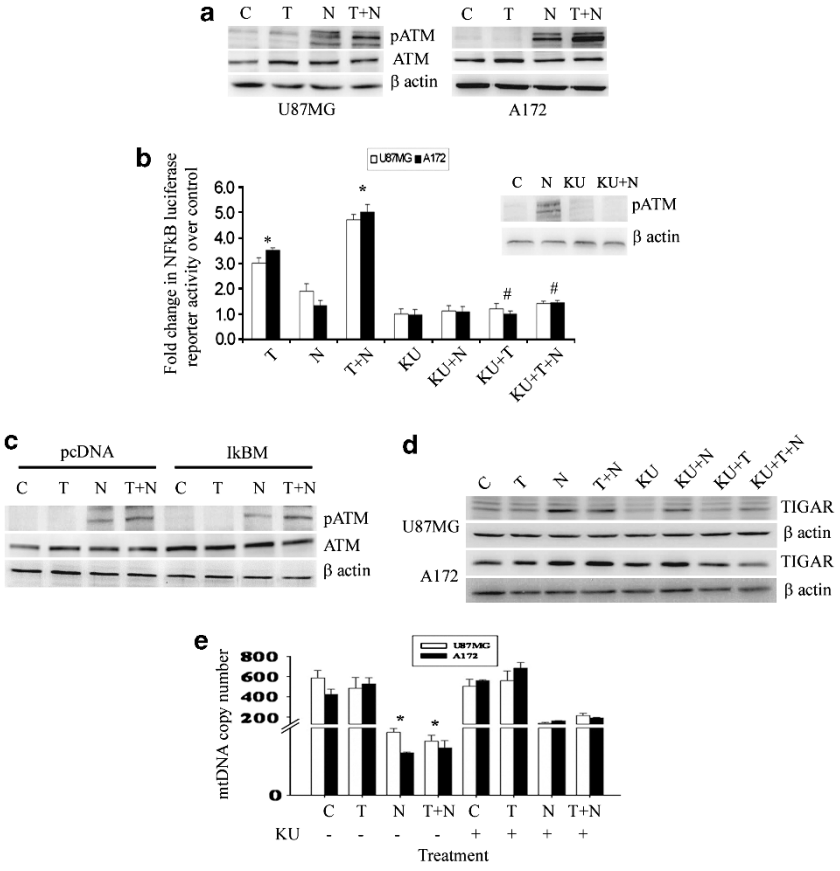

Figure 6 NCS-induced ATM phosphorylation regulates NFκB and TIGAR. (**a**) Western blot indicating increased ATM phosphorylation in cells treated with NCS both in the presence and absence of TNFα. (**b**) ATM regulates NFκB in NCS-treated cells. NFκB transcriptional activity in cells transfected with NFκB luciferase reporter construct and treated with different combinations of NCS, TNFα and ATM inhibitor Ku60019. The graph represents fold change in NFκB luciferase activity over control. Values mean ± S.E.M. from three independent experiments. *denotes significant change from control ($P<0.05$), #denotes significant change from TNFα and NCS + TNFα ($P<0.05$). Inset shows pATM levels in cells treated with NCS in the presence and absence of ATM inhibitor, as determined by western blot. (**c**) ATM phosphorylation in NCS-treated cells is independent of NFκB. Western blot demonstrating ATM phosphorylation in cells transfected with IκBM and treated with NCS in the presence and absence TNFα. (**d**) ATM regulates TIGAR in NCS and TNFα cotreated cells. Western blot demonstrating TIGAR levels in cells treated with NCS or TNFα or both in the presence of KU60019. Figures (**a**, **c**, **d**) are representative of three independent experiments. Blots were reprobed for β-actin to establish equivalent loading. (**e**) NCS reduces mitochondrial genome content. The graph represents mtDNA copy number per cell by comparing nuclear genes to the corresponding mitochondrial genes, as determined by qRT-PCR. Values represent the mean ± S.E.M. from two independent experiments. *denotes significant change from control ($P<0.05$)

ATM sustains NFκB activation.[20] However, NCS-induced ATM activation occurs independently of NFκB; as pATM levels in NCS-treated cells both in the presence and absence of TNFα were comparable between mock and IκBM-transfected cells (Figure 6c).

TNFα affects the ability of ATM to regulate TIGAR. As our findings suggest that ATM regulates NFκB, and as NFκB regulates NCS-induced TIGAR, the role of ATM in regulating TIGAR was investigated. ATM inhibition abrogated TIGAR levels in cells cotreated with NCS and TNFα (Figure 6d), suggesting that the ability of ATM to regulate TIGAR is modulated by TNFα.

NCS decreases mitochondrial copy number in an ATM independent manner. Reduction of the mitochondrial genome content induces Erk and Akt activation,[38] and ATM is involved in mitochondrial homeostasis.[39] As NCS-mediated death involved mitochondria and aberrant Erk/Akt activation, the effect of NCS-induced ATM phosphorylation on mitochondrial copy number was determined. Mitochondrial genome copy number/cell was significantly reduced upon NCS treatment both in the presence and absence of TNFα (Figure 6e). The ability of ATM inhibitor to revert NCS-mediated decrease in mitochondrial copy number both in the presence and absence of TNFα was not significant (Figure 6e).

TIGAR regulates DDR. ATM activated in response to DSBs phosphorylates H2AX.[40] γH2AX formation in the chromatin surrounding DSBs can be visualized as discrete nuclear foci.[41] Moreover, NCS-induced ROS induction is partly mediated by increasing γH2AX.[9] As NCS-induced TIGAR induction is ATM dependent and is accompanied by elevated ROS, γH2AX levels in cells transfected with TIGAR-TM and treated with different combinations of NCS and TNFα were determined. NCS increased γH2AX in the presence and absence of TNFα.This increase in γH2AX was TIGAR dependent, as elevated γH2AX levels were abrogated to control levels in TIGAR-TM-transfected cells (Figure 7a). Also, increased γH2AX foci formation seen in NCS-treated

cells both in the presence and absence of TNFα was abrogated in TIGAR-TM-transfected cells (Figure 7b).

NCS regulates genes associated with glucose metabolism. NCS-induced decreased lactate production was accompanied by increased TIGAR, which is a known p53 inducible regulator of glycolysis. As decreased lactate production and elevated TIGAR levels in NCS-treated cells suggested an altered metabolic state, the status of genes associated with glucose metabolism was analyzed in

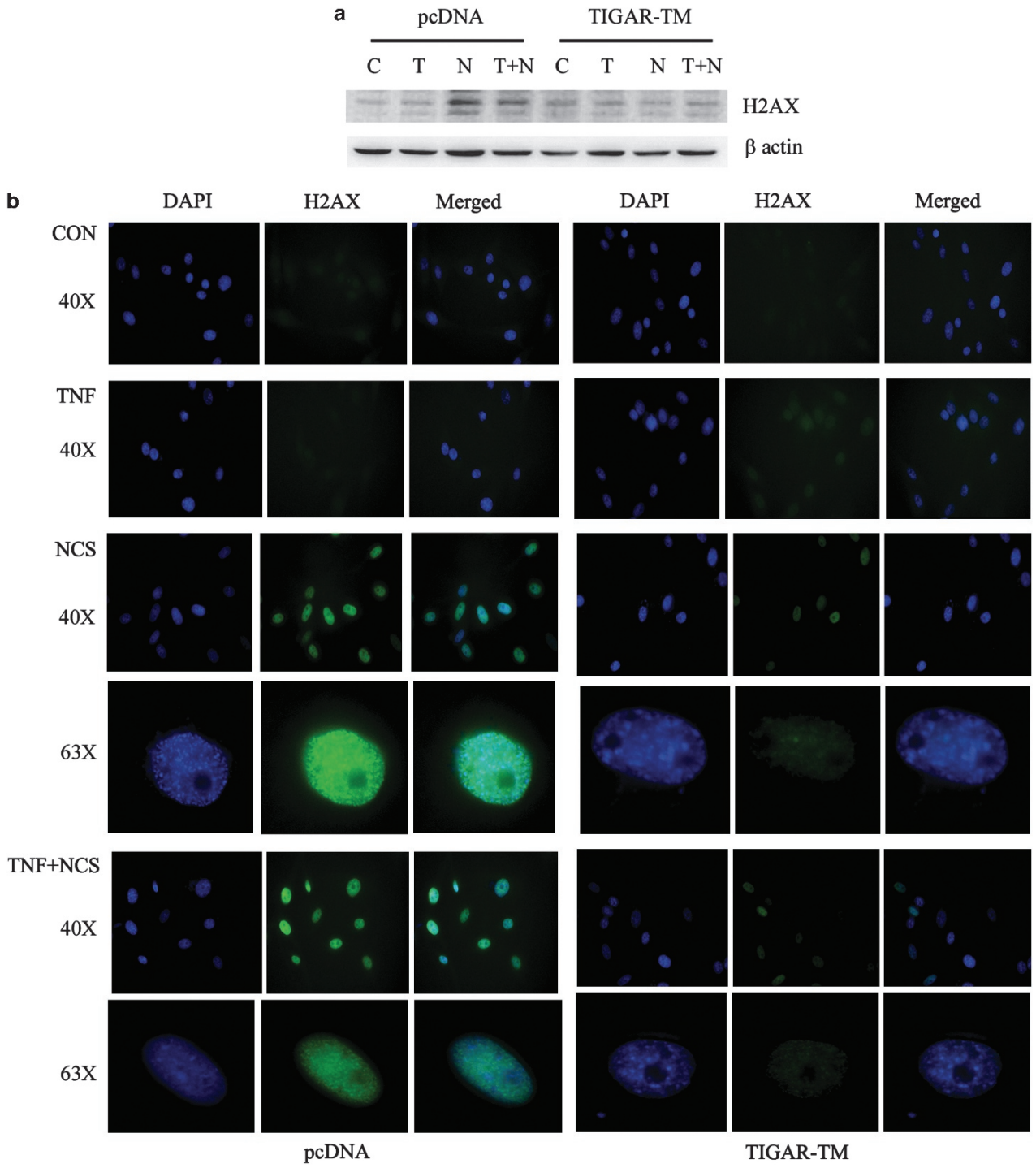

Figure 7 TIGAR regulates γH2AX expression and foci formation in NCS-treated cells. (**a**) TIGAR regulates NCS-induced γH2AX phosphorylation. Western blot demonstrates γH2AX levels in U87MG cells transfected with TIGAR-TM and treated with NCS in the presence and absence of TNFα, as compared with mock transfected control. The figure is representative of three independent experiments. Blots were reprobed for β-actin to establish equivalent loading. (**b**) TIGAR-TM abrogates γH2AX foci formation in NCS-treated cells. Immuno-cytochemistry staining for γH2AX phosphorylation (Ser 139, green) in U87MG cells transfected with TIGAR-TM and treated with NCS in the presence and absence of TNFα. DNA counterstaining was done with DAPI (blue)

Table 1 Quantitative real-time PCR to evaluate the relative transcript levels of a panel of genes associated with glucose metabolism in cells treated with NCS or TNFα or both (Fold Change over control)

Gene	TNFα	NCS	NCS + TNFα
ACLY	−1.6947	−2.4351	−3.7477
ACO1	2.7207	−1.6575	1.0417
AGL	−1.4349	−2.856	−4.0869
ALDOB	1.2092	10.5268	9.8423
ALDOC	−2.1302	−2.6372	−4.7932
FBP1	1.2346	118.2749	124.8455
FBP2	−1.1065	17.0417	14.3105
FH	1.0785	−2.856	−2.16
G6PC	8.598	42.9921	33.8011
GALM	−1.4651	−2.2799	−4.4414
GBE1	1.0381	−5.0595	−5.5443
GCK	−1.1942	2.7435	2.7019
GYS1	2.0195	−2.0477	−1.6426
GYS2	1.2346	7.7866	7.4591
HK2	1.0636	−2.7972	−3.7218
HK3	2.5829	10.8981	6.7225
IDH1	−1.455	−1.8455	−3.0126
IDH2	1.3938	−3.147	−3.1296
PC	1.6403	−1.5199	−2.2361
PCK1	3.7685	30.0856	18.1765
PDK1	1.0028	−6.653	−5.7002
PDK2	−1.8289	−1.4035	−3.6075
PDK3	1.0028	−4.8366	−6.1946
PDK4	−4.9795	−1.1599	−2.1376
PGK1	−1.5433	−3.0504	−3.1844
PGK2	1.8013	3.62	2.0691
PGM3	−1.2535	−3.061	−2.8999
PHKA1	−6.8258	−2.6463	−4.6622
PHKB	−1.2932	−3.9014	−5.0315
PHKG1	−2.145	−2.0835	−4.5347
PRPS1L1	2.5298	35.0417	31.5376
PYGM	2.4099	17.2198	16.156
SUCLG2	−1.5757	−8.3629	−9.4873
UGP2	1.2825	−2.9059	−1.9132

Abbreviation: NCS, neocarzinostatin; TNFα, tumor necrosis factor-α.
Gene expression profiling of mRNA isolated from U87MG-glioma cells treated with TNFα in the presence and absence of NCS, was analyzed by qRT-PCR for genes involved in glucose metabolism. Expressions of several genes affected by the treatments are shown. Table represents the average data from two independent experiments.

NCS-treated cells using qRT-PCR based metabolism gene array (Table 1). An increase in Fructose-1, 6 bisphosphatase (FBPase-1 and 2) levels in NCS-treated cells both in the presence and absence of TNFα was observed. This was interesting as FBPase-2 lowers fructose-2,6-bisphosphate- an inhibitor of fructose-1,6-bisphosphatase (FBPase-1), thereby enhancing the activity of FBPase-1 to inhibit glycolysis. Also, the decreased level of Hexokinase 2 (HK2), which regulates aerobic glycolysis and is involved in glioma progression,[16] suggested altered glycolysis in NCS-treated cells both in the presence and absence of TNFα (Table 1).

Discussion

The ability of radiation induced NFκB-TNFα-NFκB positive feed forward cycle to facilitate radioprotection and survival advantage, links NFκB-TNFα cross-talk to resistance and relapse of neuroblastoma following radiation therapy.[7] While radiotherapy is the mainstay of GBM treatment; survival and adaptation of cells that escape death following radiotherapy is essential for glioma promotion and progression. Constitutive activation of NFκB in GBM facilitates tumorigenesis.[42] As inhibition of NFκB activation sensitizes glioma cells to TNFα-induced apoptosis,[21,22] we investigated whether TNFα could affect the responsiveness of glioma cells to radiomimetics such as NCS. Though TNFα enhanced NCS-induced glioma cell death, the response of cells to radiomimetic NCS in the presence of TNFα is paradoxical as the activation of NFκB and Akt/Erk associated with prosurvival response is concurrent with apoptosis. Enhanced apoptosis in NCS and TNFα cotreated cells upon NFκB inhibition, indicates that NCS-induced NFκB enhances cell survival to subsequently limit its therapeutic potential; as reported previously with radiation therapy.[7] This ability of NCS-induced prosurvival NFκB and Akt to prevent manifestation of the death inducing ability of NCS to the fullest, could possibly account for the non-linear dose-dependent response of glioma cells to NCS.

NCS-induced proapoptotic TIGAR is dependent on NFκB activation and this dependence is further heightened in the presence of proinflammatory TNFα. As elevated NFκB and Akt activation maximizes survival of NCS-treated cells, increase in TIGAR possibly occurs to counteract these prosurvival signals. Though Akt activation leads to Warburg effect, high Akt activity can also render cells sensitive to death induced by glycolysis inhibitor.[43] NCS-induced Akt activation could possibly sensitize glioma cells to TIGAR – an inhibitor of glycolysis. NFκB promotes metabolic adaptation in cancer,[18] and p53 prevents NFκB activation through suppression of glycolysis.[44] Although NFκB activation in TNFα and NCS cotreated cells is TIGAR independent, p53 induction in these cells is regulated by TIGAR. It is possible that TIGAR-dependent p53 regulates NFκB activation through suppression of glycolysis, Taken together, it is the fine tuning between pro- and antiapoptotic responses (TIGAR *versus* Akt/NFκB), that enable glioma cells to withstand radiomimetic-induced stress and acquire radioresistance or undergo death.

DSB (double-strand breaks) trigger ATM- and Akt-dependent Erk prosurvival signal,[45] and ATM/ERK/NFκB prosurvival network induces radio-adaptive response in human keratinocytes.[46] The ability of NCS-induced ATM to regulate NFκB in glioma cells exposed to radiomimetics, agrees with previous reports that ATM inhibition radiosensitizes glioma cells.[36] This coupled with ATM-NFκB axis driven TIGAR to regulate Akt/Erk activation negatively and γH2AX activation positively, suggests that a feedback regulatory mechanism functions as a rheostat to affect radiomimetic-induced adaptive responses (Figure 8). Previous studies have shown that irradiation induced TGF-β signaling triggers complicated negative feedback regulation to affect irradiation induced adaptive responses, genomic instability and bystander effects.[47] Though NFκB can affect the death inducing potential of NCS via regulation of proapoptotic TIGAR; its own prosurvival and cytoprotective ability under such conditions can concurrently dampen TIGAR-induced cell death. Cells that survive radiation-induced injury contribute to glioma radioresistance through increase in DNA repair capacity.[48] Importantly, acquisition of proinflammatory cytokine inducible NFκB activity in TNFα selected breast cancer cells, promotes resistance to irradiation without affecting transformation.[8] It is tempting to speculate that increased NFκB activation in

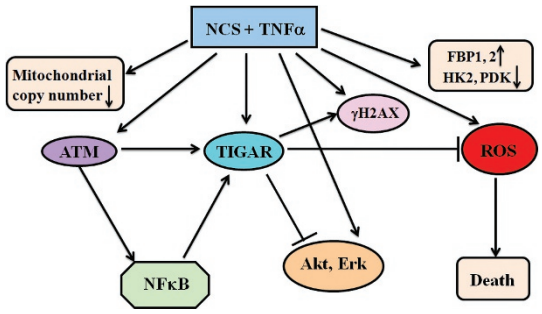

Figure 8 Proposed model demonstrating the regulation of TIGAR and its role in the responsiveness of glioma cells to radiomimetics in the presence of TNFα. NCS induces TIGAR in an ATM- and NFκB-dependent manner. NCS-mediated glioma cell death is ROS dependent and TIGAR regulates ROS generation in addition to Akt/Erk activation and γH2AX foci formation. NCS-induced alteration in genes associated with glycolysis is affected by the presence of TNFα. FBP, Fructose Bisphosphatase 2; HK2, Hexokinase 2; PDK, Pyruvate dehydrogenase kinase

cells that survives in the NCS-TNFα milieu could contribute to tumor recurrence with a resistant phenotype.

ATM stimulates pentose phosphate pathway (PPP) to induce anti-oxidant defense, and ATM-mediated inhibition of glycolysis has been suggested to reduce ROS, generated through glycolytic metabolism.[49] As TIGAR activates PPP,[13] ATM-driven TIGAR could regulate redox homeostasis in NCS-treated cells by preventing excessive ROS generation. p53 protects genome from oxidative damage by decreasing ROS levels[50] and NCS-induced p53 and ROS is regulated by TIGAR. Misrepair of radiation-induced DSBs can be mutagenic. By functioning as sensor that detects DNA damage, TIGAR likely protects cells from ROS-associated DNA damage that could lead to genomic instability. The simultaneous increase in antiapoptotic Akt and proapoptotic ROS in cells transfected with TIGAR-TM, is concurrent with its ability to rescue cells from NCS-induced death. This dichotomous behavior of TIGAR-TM coupled with its ability to decrease both p53 and p21 levels, could possibly account for reversal of NCS-mediated death in TIGAR-TM-transfected cells despite elevated ROS generation.

NFκB represses mitochondrial gene expression following TNFα stimulation[51] and mitochondrial dysfunction is associated with apoptosis.[52] NCS-induced decreased mitochondrial copy number and loss of mitochondrial integrity could have also resulted in increased Akt activation, as mitochondrial DNA deletion increases NADH-dependent Akt activation that contributes to drug resistance.[28] Increased FBPase-1 and 2 levels concurrent with elevated TIGAR indicated altered glycolysis in NCS-treated cells. As cancer cells use increased glycolysis to generate ATP as main energy source,[53] abrogated ATP generation in NCS-treated cells was concomitant with decreased glycolysis. TNFα also affected NCS-mediated regulation of several genes associated with glucose metabolism such as Aldolase C, Phospho-enolpyruvate carboxykinase 1, Pyruvate dehydrogenase kinase and Phosphorylase kinase.

Through simultaneous regulation of cytoprotective NFκB and pro-apoptotic TIGAR, ATM balances resistance *versus* sensitivity to radiomimetics. Here we demonstrate the importance of ATM-NFκB axis in regulating responsiveness of glioma cells to radiomimetic through metabolic modeler TIGAR in a proinflammatory milieu. Given that metabolic modulation holds promise as a potential antiglioma therapeutic approach,[17] understanding mechanisms of TIGAR regulation to subsequently sensitize glioma cells to apoptosis warrants investigation. As glioma cells that escape NCS-induced death could acquire concurrent adaptation and survival advantage through NFκB and Akt/Erk activation; further investigation of this complex regulation of pro/antisurvival mediators and metabolic remodeling following exposure to radiomimetics, would lead to better understanding of radioresistance and open avenues for improving efficacy of glioma radiotherapy.

Materials and Methods

Processing of tissue and Immunohistochemistry. Immunohistochemistry was performed on histologically confirmed GBM ($n=21$) to determine TIGAR expression as described.[54] Non-neoplastic brain tissue ($n=8$) from margins of the tumors was used as control. Samples were obtained as per the guidelines of Institutional Human Ethics Committee of NBRC.

Cell culture and treatment. Glioblastoma cell lines A172 and U87MG obtained from American Type Culture Collection (ATCC, Manassas, VA, USA) were cultured in DMEM supplemented with 10% fetal bovine serum. On attaining semi-confluence, cells were switched to serum free media (SFM) and after 12 h, cells were treated with different combinations of NCS (Sigma, St. Louis, MO, USA) and TNFα (R&D Systems, Minneapolis, MN, USA; 50 ng/ml) in the presence and absence of Caspase-9 inhibitor (Calbiochem, Merck KGaA, Darmstadt, Germany), or AKT inhibitor LY294002 or ATM inhibitor KU60019 (Tocris Bioscience, Northpoint, UK) for 24 h. All reagents were purchased from Sigma unless otherwise stated.

Determination of cell viability. Viability of glioma cells treated with different combinations of TNFα and NCS in the presence and absence of 50 μM Caspase-9 inhibitor or 10 μM LY294002 or 5 μM KU60019, for 24 h was assessed using the MTS assay (Promega, Madison, WI, USA) as described.[22] Similarly, the viability of cells transfected with TIGAR siRNA (40 nM), TIGAR-WT or TIGAR-TM and treated with TNFα or NCS or both for 24 h was assessed using the MTS assay as described.[22] Values were expressed as a percentage relative to those obtained in controls.

Western blot analysis. Protein was isolated from cells treated with different combinations of TNFα, NCS, LY294002 and KU60019, and western blot was performed as described.[55] The following antibodies were used – p53, $_{p}$p53 ser-15, p21 (BD Biosciences, San Diego, CA, USA), BAX, BAD, Cytochrome *c*, Caspase-9 (Abcam, Cambridge, UK), γH2AX (Ser 139) (Upstate, Millipore, Temecula, CA, USA), TIGAR (Novus, Cambridge science Park, Cambridge, UK), ATM and pATM. LC3-I/II, Akt, pAkt, Erk, pErk were obtained from Cell Signaling (Danvers, MA, USA). Antibodies were purchased from Santa Cruz Biotechnology (Santa Cruz, CA, USA) unless otherwise mentioned. Secondary antibodies were purchased from Vector Laboratories (Burlingame, CA, USA). The blots were stripped and reprobed with anti-β-actin (Sigma) to determine equivalent loading as described.[55]

Transfections and luciferase assay. Reporter assay was performed in cells transfected with NFκB luciferase reporter alone or cotransfected with TIGAR-TM construct and treated with different combinations of TNFα, NCS and KU60019, as described previously.[54] In experiments with TIGAR-TM and DN-NFκB (IκBM), control transfection using the appropriate empty vector construct was performed as described.[22] For siRNA-mediated knockdown experiment, cells were transfected with 40 nmol/l TIGAR or non-specific siRNA (Dharmacon, Thermo Fischer Scientific, Lafayette, CO, USA) using Lipofectamine RNAi Max reagent (Life Technologies-Invitrogen, Carlsbad, CA, USA) as described.[22] Western blot was performed on protein isolated from cells transfected with TIGAR-TM or IκBM and treated with different combinations of TNFα and NCS for 24 h as described.[55] The NFκB luciferase reporter and DN-NFκB (IκBM) were purchased from Clontech (Madison, WI, USA). We thank Karen Vousden for providing

the pcdna3.1FLAG-TIGAR and pcdna3.1FLAG-TIGAR-TM mutant expression plasmids.[13] TIGAR-TM is a triple mutant, altered in three key residues essential for bisphosphatase activity.[13]

Measurement of intracellular ATP. Intracellular ATP levels were measured by luminometric assay using the ATPlite, Luninescence ATP detection assay system (Perkin Elmer, Waltham, MA, USA) according to the manufacturer's instructions. Briefly, cells treated with different combination of TNFα and NCS for 24 h in 96-well plates were lysed with 50 μl of mammalian cell lysis solution, incubated with 50 μl substrate solution (Luciferase/luciferin) for 10 min in dark, and luminescence was measured (Glomax luminometer, Promega). Values were expressed as a percentage relative to those obtained in controls.

Lactate measurement. Lactate release in the supernatant collected from cells treated with different combinations of NCS and TNFα for 24 h, was measured with a Lactate Colorimetric Assay Kit (Biovision Inc. Milpitas Blvd, CA, USA), according to the manufacturer's indication. Briefly, 5 μl of supernatant was incubated with reaction mix containing lactate assay buffer, lactate probe and lactate enzyme mix for 30 min in dark. OD was measured at 570 nm, and concentration of lactate (nmol/μl) was measured using standard curve.

qRT-PCR of the mitochondrial genome content. The mitochondrial Novaquant human mitochondrial to nuclear DNA ratio kit genome content was used for determining mtDNA copy number according to manufacturer's instructions (NovaQUANT, Merck KGaA). Briefly, genomic DNA isolated from test samples were mixed with qRT-PCR master mix and plated on provided qRT-PCR plate containing a set of four optimized PCR primer pairs targeting two nuclear and two mitochondrial genes. Resultant C_t values obtained from RT-PCR were used to represent mtDNA copy number per cell by comparing nuclear genes to the corresponding mitochondrial genes.

Immunofluorescence. Following treatment with NCS in the presence and absence of TNFα for 24 h, cells were fixed in 4% paraformaldehyde. Fixed cells were incubated with anti-γH2AX antibody overnight at 4 °C, washed and further incubated with Alexa Fluor 488 (Invitrogen) secondary antibody for 2 h at room temperature. The expression of γH2AX (green) was analyzed using Zeiss ApoTome Imager.Z1 as described.[56] DNA counterstaining was performed with 4,6-diamidino-2-phenylindole (DAPI) (Vector).

For MitoTracker Green FM (Invitrogen) staining, cells treated with NCS or TNFα or both in SFM for 24 h were incubated with 500 nM of Mitotracker probe prepared in prewarmed (37 °C) SFM and incubated for 45 min at 37 °C. After incubation, staining media was replaced with fresh prewarm PBS and images were taken under fluorescence microscope.

Measurement of ROS. Intracellular ROS generation was assessed using fluorescent dye dihydroethidium (DHE, Sigma) as described.[11] For detection with DHE, mock and TIGAR-TM transfected cells treated with different combination of NCS and TNFα for 24 h were loaded with 1 μM DHE at 37 °C for 20 min and images ware captured by Nikon Eclipse TS100 (Nikon Instruments Inc., Melville, NY, USA) fluorescence microscope using a Rhodamine filter.

Human metabolism qRT-PCR array. qRT-PCR was performed using The Human Glucose Metabolism RT2 Profiler containing 84 metabolism-related genes (Qiagen, Hilden, Germany) as described previously.[22] Five housekeeping genes were included on the array (B2M, HPRT1, RPL13A, GAPDH and ACTB) to normalize the transcript levels. Results were analyzed as per user manual guidelines using integrated web-based software package for the PCR Array System (RT2 Profiler PCR Array Human Glucose Metabolism PAHS-006Z).

Statistical analysis. All comparisons between groups were performed using two-tailed paired student's *t*-test. All *P*-values < 0.05 were taken as significant.

Conflict of Interest

The authors declare no conflict of interest.

Acknowledgements. The work was supported by a research grant from the Department of Biotechnology (DBT, Government of India no. BT/PR/12924/Med/30/235/2009) to ES.

1. Brach MA, Hass R, Sherman ML, Gunji H, Weichselbaum R, Kufe D. Ionizing radiation induces expression and binding activity of the nuclear factor kappa B. *J Clin Invest* 1991; **88**: 691–695.
2. Iwanaga M, Mori K, Iida T, Urata Y, Matsuo T, Yasunaga A *et al.* Nuclear factor kappa B dependent induction of gamma glutamylcysteine synthetase by ionizing radiation in T98G human glioblastoma cells. *Free Radic Biology Med* 1998; **24**: 1256–1268.
3. Tsujimoto M, Yip YK, Vilcek J. Tumor necrosis factor: specific binding and internalization in sensitive and resistant cells. *Proc Natl Acad Sci USA* 1985; **82**: 7626–7630.
4. Beg AA, Baltimore D. An essential role for NF-kappaB in preventing TNF-alpha-induced cell death. *Science* 1996; **274**: 782–784.
5. Wang CY, Mayo MW, Baldwin AS Jr.. TNF- and cancer therapy-induced apoptosis: potentiation by inhibition of NF-kappaB. *Science* 1996; **274**: 784–787.
6. Ivanov VN, Fodstad O, Ronai Z. Expression of ring finger-deleted TRAF2 sensitizes metastatic melanoma cells to apoptosis via up-regulation of p38, TNFalpha and suppression of NF-kappaB activities. *Oncogene* 2001; **20**: 2243–2253.
7. Veeraraghavan J, Natarajan M, Aravindan S, Herman TS, Aravindan N. Radiation-triggered tumor necrosis factor (TNF) alpha-NFkappaB cross-signaling favors survival advantage in human neuroblastoma cells. *J Biol Chem* 2001; **286**: 21588–21600.
8. Braunstein S, Formenti SC, Schneider RJ. Acquisition of stable inducible up-regulation of nuclear factor-kappaB by tumor necrosis factor exposure confers increased radiation resistance without increased transformation in breast cancer cells. *Mol Cancer Res* 2008; **6**: 78–88.
9. Kang MA, So EY, Simons AL, Spitz DR, Ouchi T. DNA damage induces reactive oxygen species generation through the H2AX-Nox1/Rac1 pathway. *Cell Death Dis* 2012; **3**: e249.
10. Sharma V, Joseph C, Ghosh S, Agarwal A, Mishra MK, Sen E. Kaempferol induces apoptosis in glioblastoma cells through oxidative stress. *Mol Cancer Ther* 2007; **6**: 2544–2553.
11. Dixit D, Sharma V, Ghosh S, Koul N, Mishra PK, Sen E. Manumycin inhibits STAT3, telomerase activity, and growth of glioma cells by elevating intracellular reactive oxygen species generation. *Free Radic Biol Med* 2009; **47**: 364–374.
12. Achanta G, Huang P. Role of p53 in sensing oxidative DNA damage in response to reactive oxygen species-generating agents. *Cancer Res* 2004; **64**: 6233–6239.
13. Bensaad K, Tsuruta A, Selak MA, Vidal MN, Nakano K, Bartrons R *et al.* TIGAR, a p53-inducible regulator of glycolysis and apoptosis. *Cell* 2006; **126**: 107–120.
14. Pena-Rico MA, Calvo-Vidal MN, Villalonga-Planells R, Martinez-Soler F, Gimenez-Bonafe P, Navarro-Sabate A *et al.* TP53 induced glycolysis and apoptosis regulator (TIGAR) knockdown results in radiosensitization of glioma cells. *Radiother Oncol* 2011; **101**: 132–139.
15. Wanka C, Steinbach JP, Rieger J. Tp53-induced glycolysis and apoptosis regulator (TIGAR) protects glioma cells from starvation-induced cell death by upregulating respiration and improving cellular redox homeostasis. *J Biol Chem* 2012; **287**: 33436–33446.
16. Wolf A, Agnihotri S, Micallef J, Mukherjee J, Sabha N, Cairns R *et al.* Hexokinase 2 is a key mediator of aerobic glycolysis and promotes tumor growth in human glioblastoma multiforme. *J Exp Med* 2011; **208**: 313–326.
17. Wolf A, Agnihotri S, Guha A. Targeting metabolic remodeling in glioblastoma multiforme. *Oncotarget* 2010; **1**: 552–562.
18. Mauro C, Leow SC, Anso E, Rocha S, Thotakura AK, Tornatore L *et al.* NF-kappaB controls energy homeostasis and metabolic adaptation by upregulating mitochondrial respiration. *Nat Cell Biol* 2011; **13**: 1272–1279.
19. Bar-Shira A, Rashi-Elkeles S, Zlochover L, Moyal L, Smorodinsky NI, Seger R *et al.* ATM-dependent activation of the gene encoding MAP kinase phosphatase 5 by radiomimetic DNA damage. *Oncogene* 2002; **21**: 849–855.
20. Piret B, Schoonbroodt S, Piette J. The ATM protein is required for sustained activation of NF-kappaB following DNA damage. *Oncogene* 1999; **18**: 2261–2271.
21. Gupta P, Dixit D, Sen E. Oncrasin targets the JNK-NF-kappaB axis to sensitize glioma cells to TNFalpha-induced apoptosis. *Carcinogenesis* 2012; **34**: 388–396.
22. Dixit D, Sharma V, Ghosh S, Mehta VS, Sen E. Inhibition of Casein kinase-2 induces p53-dependent cell cycle arrest and sensitizes glioblastoma cells to tumor necrosis factor (TNFalpha)-induced apoptosis through SIRT1 inhibition. *Cell Death Dis* 2011; **3**: e271.
23. Liang Y, Yan C, Schor NF. Apoptosis in the absence of caspase 3. *Oncogene* 2001; **20**: 6570–6578.
24. Kluck RM, Bossy-Wetzel E, Green DR, Newmeyer DD. The release of cytochrome c from mitochondria: a primary site for Bcl-2 regulation of apoptosis. *Science* 1997; **275**: 1132–1136.
25. Sattler UG, Meyer SS, Quennet V, Hoerner C, Knoerzer H, Fabian C *et al.* Glycolytic metabolism and tumour response to fractionated irradiation. *Radiother Oncol* 2010; **94**: 102–109.
26. Lemire J, Mailloux RJ, Appanna VD. Mitochondrial lactate dehydrogenase is involved in oxidative-energy metabolism in human astrocytoma cells (CCF-STTG1). *PloS one* 2008; **3**: e1550.

27. Madrid LV, Wang CY, Guttridge DC, Schottelius AJ, Baldwin AS Jr., Mayo MW. Akt suppresses apoptosis by stimulating the transactivation potential of the RelA/p65 subunit of NF-kappaB. *Mol Cell Biol* 2000; **20**: 1626–1638.
28. Pelicano H, Xu RH, Du M, Feng L, Sasaki R, Carew JS *et al.* Mitochondrial respiration defects in cancer cells cause activation of Akt survival pathway through a redox-mediated mechanism. *J Cell Biol* 2006; **175**: 913–923.
29. Wang T, Hu YC, Dong S, Fan M, Tamae D, Ozeki M *et al.* Co-activation of ERK, NF-kappaB, and GADD45beta in response to ionizing radiation. *J Biol Chem* 2005; **280**: 12593–12601.
30. Johnson RF, Perkins ND. Nuclear factor-kappaB, p53, and mitochondria: regulation of cellular metabolism and the Warburg effect. *Trends Biochem Sci* 2012; **37**: 317–324.
31. Derdak Z, Lang CH, Villegas KA, Tong M, Mark NM, de la Monte SM *et al.* Activation of p53 enhances apoptosis and insulin resistance in a rat model of alcoholic liver disease. *J Hepatol* 2011; **54**: 164–172.
32. Vander Heiden MG, Plas DR, Rathmell JC, Fox CJ, Harris MH, Thompson CB. Growth factors can influence cell growth and survival through effects on glucose metabolism. *Mol Cell Biol* 2001; **21**: 5899–5912.
33. Bensaad K, Cheung EC, Vousden KH. Modulation of intracellular ROS levels by TIGAR controls autophagy. *EMBO J* 2009; **28**: 3015–3026.
34. Katayama M, Kawaguchi T, Berger MS, Pieper RO. DNA damaging agent-induced autophagy produces a cytoprotective adenosine triphosphate surge in malignant glioma cells. *Cell Death Differ* 2007; **14**: 548–558.
35. Viniegra JG, Martinez N, Modirassari P, Hernandez Losa J, Parada Cobo C, Sanchez-Arevalo Lobo VJ *et al.* Full activation of PKB/Akt in response to insulin or ionizing radiation is mediated through ATM. *J Biol Chem* 2005; **280**: 4029–4036.
36. Golding SE, Rosenberg E, Adams BR, Wignarajah S, Beckta JM, O'Connor MJ *et al.* Dynamic inhibition of ATM kinase provides a strategy for glioblastoma multiforme radiosensitization and growth control. *Cell Cycle* 2012; **11**: 1167–1173.
37. Wu ZH, Shi Y, Tibbetts RS, Miyamoto S. Molecular linkage between the kinase ATM and NF-kappaB signaling in response to genotoxic stimuli. *Science* 2006; **311**: 1141–1146.
38. Cook CC, Kim A, Terao S, Gotoh A, Higuchi M. Consumption of oxygen: a mitochondrial-generated progression signal of advanced cancer. *Cell Death Dis* 2012; **3**: e258.
39. Eaton JS, Lin ZP, Sartorelli AC, Bonawitz ND, Shadel GS. Ataxia-telangiectasia mutated kinase regulates ribonucleotide reductase and mitochondrial homeostasis. *J Clin Invest* 2007; **117**: 2723–2734.
40. Burma S, Chen BP, Murphy M, Kurimasa A, Chen DJ. ATM phosphorylates histone H2AX in response to DNA double-strand breaks. *J Biol Chem* 2001; **276**: 42462–42467.
41. Rogakou EP, Pilch DR, Orr AH, Ivanova VS, Bonner WM. DNA double-stranded breaks induce histone H2AX phosphorylation on serine 139. *J Biol Chem* 1998; **273**: 5858–5868.
42. Nozell S, Laver T, Moseley D, Nowoslawski L, De Vos M, Atkinson GP *et al.* The ING4 tumor suppressor attenuates NF-kappaB activity at the promoters of target genes. *Mol Cell Biol* 2008; **28**: 6632–6645.
43. Fan Y, Dickman KG, Zong WX. Akt and c-Myc differentially activate cellular metabolic programs and prime cells to bioenergetic inhibition. *J Biol Chem* 2010; **285**: 7324–7333.
44. Kawauchi K, Araki K, Tobiume K, Tanaka N. p53 regulates glucose metabolism through an IKK-NF-kappaB pathway and inhibits cell transformation. *Nat Cell Biol* 2008; **10**: 611–618.
45. Khalil A, Morgan RN, Adams BR, Golding SE, Dever SM, Rosenberg E *et al.* ATM-dependent ERK signaling via AKT in response to DNA double-strand breaks. *Cell Cycle* 2011; **10**: 481–491.
46. Ahmed KM, Nantajit D, Fan M, Murley JS, Grdina DJ, Li JJ. Coactivation of ATM/ERK/NF-kappaB in the low-dose radiation-induced radioadaptive response in human skin keratinocytes. *Free Radic Biol Med* 2009; **46**: 1543–1550.
47. Klokov D, Criswell T, Leskov KS, Araki S, Mayo L, Boothman DA. IR-inducible clusterin gene expression: a protein with potential roles in ionizing radiation-induced adaptive responses, genomic instability, and bystander effects. *Mutat Res* 2004; **568**: 97–110.
48. Bao S, Wu Q, McLendon RE, Hao Y, Shi Q, Hjelmeland AB *et al.* Glioma stem cells promote radioresistance by preferential activation of the DNA damage response. *Nature* 2006; **444**: 756–760.
49. Cosentino C, Grieco D, Costanzo V. ATM activates the pentose phosphate pathway promoting anti-oxidant defense and DNA repair. *EMBO J* 2011; **30**: 546–555.
50. Sablina AA, Budanov AV, Ilyinskaya GV, Agapova LS, Kravchenko JE, Chumakov PM. The antioxidant function of the p53 tumor suppressor. *Nat Med* 2005; **11**: 1306–1313.
51. Cogswell PC, Kashatus DF, Keifer JA, Guttridge DC, Reuther JY, Bristow C *et al.* NF-kappa B and I kappa B alpha are found in the mitochondria. Evidence for regulation of mitochondrial gene expression by NF-kappa B. *J Biol Chem* 2003; **278**: 2963–2968.
52. Suen DF, Norris KL, Youle RJ. Mitochondrial dynamics and apoptosis. *Genes Dev* 2008; **22**: 1577–1590.
53. Pelicano H, Martin DS, Xu RH, Huang P. Glycolysis inhibition for anticancer treatment. *Oncogene* 2006; **25**: 4633–4646.
54. Tewari R, Choudhury SR, Ghosh S, Mehta VS, Sen E. Involvement of TNFalpha-induced TLR4-NF-kappaB and TLR4-HIF-1alpha feed-forward loops in the regulation of inflammatory responses in glioma. *J Mol Med (Berl)* 2012; **90**: 67–80.
55. Sharma V, Dixit D, Koul N, Mehta VS, Sen E. Ras regulates interleukin-1beta-induced HIF-1alpha transcriptional activity in glioblastoma. *J Mol Med (Berl)* 2011; **89**: 123–136.
56. Ghildiyal R, Dixit D, Sen E. EGFR inhibitor BIBU induces apoptosis and defective autophagy in glioma cells. *Molecular carcinogenesis* 2012; doi: 10.1002/mc.21938.

Cell Death and Disease **is an open-access journal published by** ***Nature Publishing Group*****. This work is licensed under a Creative Commons Attribution-NonCommercial-NoDerivs 3.0 Unported License. To view a copy of this license, visit http://creativecommons.org/licenses/by-nc-nd/3.0/**

Supplementary Information accompanies this paper on Cell Death and Disease website (http://www.nature.com/cddis)